

¹ Insertion Approach: Bolstering the Reproducibility of ² Electrochemical Signal Amplification via DNA Superstructures

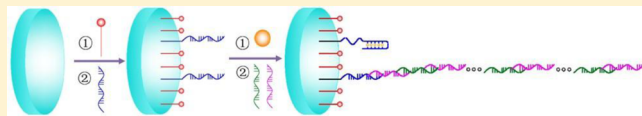
³ Li Yang,^{†,‡} Caihua Zhang,^{†,‡} Hong Jiang,[‡] Guijuan Li,^{*,†} Jiahai Wang,^{*,‡} and Erkang Wang^{*,‡}

⁴ [†]College of Chemical Engineering, Changchun University of Technology, Changchun, Jilin 130012, China

⁵ [‡]State Key Laboratory of Electroanalytical Chemistry, Changchun Institute of Applied Chemistry, Chinese Academy of Science, Changchun, Jilin 130022, China

⁷ Supporting Information

ABSTRACT: For more than a decade, the backfilling approach for the immobilization of DNA probes has been routinely adopted for the construction of functional interfaces; however, reliably reproducing electrochemical signal amplification by this method is a challenge. In this research, we demonstrate that the insertion approach significantly bolsters the reproducibility of electrochemical signal amplification via DNA superstructures. The combination of the backfilling approach and the DNA superstructure formation poses a big challenge to reliably reproducing electrochemical signal amplification. In order to use the detection of Hg^{2+} as a prototype of this new strategy, a thymine-rich DNA probe that is specific to mercury ion was applied in this study. The presence of Hg^{2+} induces the folding of the DNA probes and inhibits the formation of DNA superstructures. By using electroactive probes ($[Ru(NH_3)_6]^{3+}$) that are electrostatically adsorbed onto the double strands, differential pulse voltammetry (DPV) could quantitatively confirm the presence of Hg^{2+} . A limit of detection (LOD) and a limit of quantification (LOQ) (LOQ) as low as 0.3 and 9.5 pM, respectively, were achieved. Furthermore, excellent selectivity and real sample analysis demonstrated the promising potential of this approach in future applications.



The self-assembly of DNA monolayers on gold electrodes is a topic of great interest for the electrochemical sensor community.¹ For more than a decade, the backfilling approach, which entails the shoehorning of an alkanethiol into the void spaces between constituents of a preassembled DNA monolayer, has become the mainstream.^{2–4} Despite the tremendous progress achieved in this field, the reproducibility of electrochemical signals from DNA-modified electrodes still merits further investigation. One concern that prompts additional study is the competitive binding of the alkanethiols and DNA thiol groups to the gold surface, leading to the diffusion of the DNA probes along the surface and the formation of aggregated domains. Consequently, the interprobe distance among the DNAs in the monolayer becomes inhomogeneous, with smaller spacings in the aggregated domains than the average interprobe distance calculated from measurements via the ensemble techniques. The uncontrollable heterogeneity caused by local aggregation^{5,6} is unfavorable for the reproducibility of the signal amplification via large nano/microstructures; instead, the signal amplification prefers low probe density. To achieve optimal low-probe density and avoid uncontrollable heterogeneity, strict control over experimental operations to construct reproducible electrochemical biosensors is required.

Suitable signal amplification in these electrochemical sensors has been achieved through the use of DNA superstructures, which consist of long DNA polymers hybridized from two single stranded DNAs that have partially complementary segments.⁷ When the backfilling approach is used in combination with a DNA superstructure, electrochemical sensors show large electro-

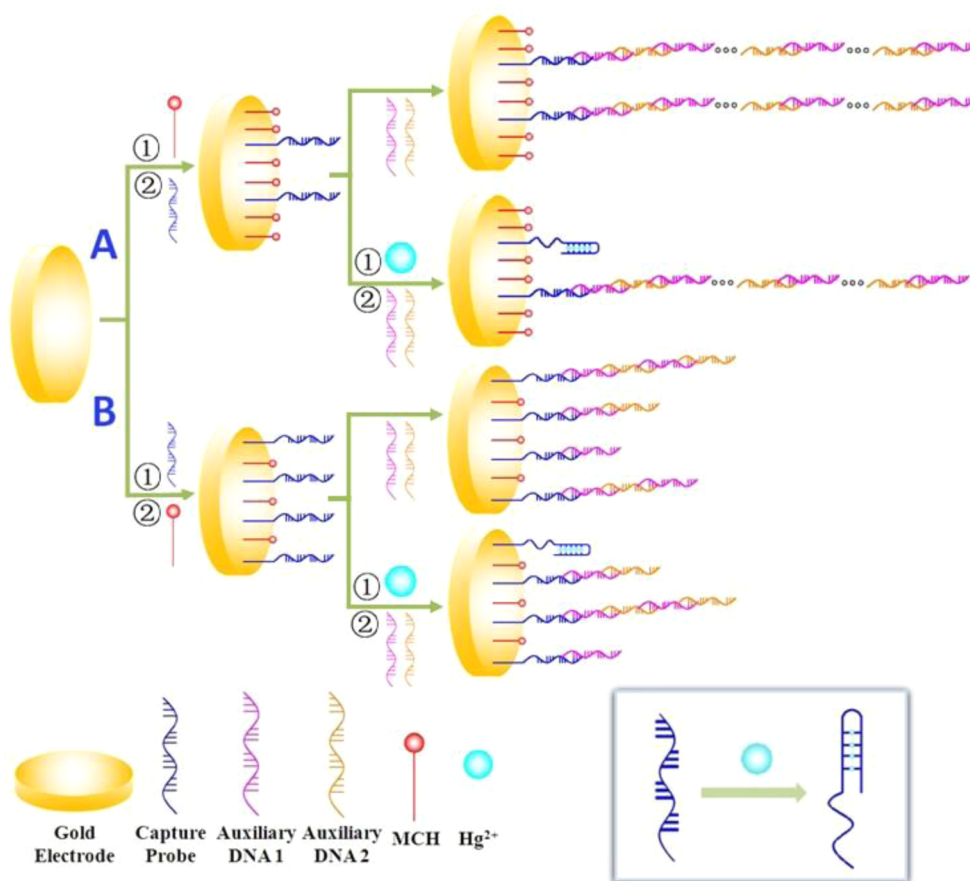
chemical signal variations. To improve sensor quality in terms of hybridization efficiency and reproducibility, a monolayer with large void spaces between each DNA probe is required to eliminate the steric impedance and electrostatic repulsion between each superstructure.^{8–12} Most recently, monolayers formed via the insertion approach, in which thiol moiety-labeled DNA is inserted into a loosely packed alkane monolayer, have met the above-mentioned requirement and have been systematically investigated by atomic force microscopy (AFM).¹³ As compared with the backfilling approach, DNA probes can be inserted into an alkane monolayer at lower surface density,¹⁴ which is highly advantageous for combination with DNA superstructures.

To date, no electrochemical sensor based on the combination of the insertion approach and DNA superstructures has been proposed. In this study, the distinct features of this concept were investigated, using the detection of Hg^{2+} as a sample case. Mercury ions are common heavy metal pollutants in the environment, and although toxic to humans, they can be consumed by bacteria. Further biological accumulation through the food chain imperils human health. Even low concentrations in the kidneys, hematopoietic system, or liver can result in serious consequences.^{15–17} Therefore, the establishment of highly selective and sensitive methods to detect Hg^{2+} would be significant. Heretofore, the most commonly used techniques

Received: January 3, 2014

Accepted: April 24, 2014

Scheme 1. Schematic Illustration for Detecting Mercury Ions Based on Electrochemical Signal Amplification by DNA Superstructures in Combination with (A) the Insertion Approach and (B) the Backfilling Approach^a



^aThe capture probe forms thymine- Hg^{2+} -thymine complexes in the presence of Hg^{2+} .

for Hg^{2+} detection have been atomic absorption spectrometry (AAS),^{18,19} cold-vapor atomic fluorescence spectroscopy (CV-AFS),^{20,21} inductively coupled plasma-mass spectrometry (ICPMS),²² inductively coupled plasma-atomic emission spectrometry (ICP-AES),²³ and surface-enhanced Raman scattering (SERS)²⁴ sensing. Although these techniques are sensitive and accurate for assaying Hg^{2+} , most rely on costly instruments with time-consuming procedures and are unsuitable for real field analysis. In recent years, although several electrochemical sensors have been constructed and shown to exhibit high sensitivity, their preparations have been based on the backfilling approach.^{25,26}

In this study, we exploit a specific thymine- Hg^{2+} -thymine (T- Hg^{2+} -T) coordination: T-rich DNA probes immobilized on a gold electrode via the insertion approach can fold into hairpin structures in the presence of mercury ions, blocking further DNA polymer extension. The decrease in the current observed by differential pulse voltammetry (DPV) can be used to quantitatively determine the presence of Hg^{2+} . The DNA superstructures that grow from the probes on the electrode significantly amplify the change in the current peak. This new protocol for the construction of electrochemical sensors can provide reproducible electrochemical signals. Label-free detection is another advantage for our proposed scenario, which utilizes an electroactive complex ($[\text{Ru}(\text{NH}_3)_6]^{3+}$) as a signaling molecule that binds to the anionic phosphate backbone of DNA strands via electrostatic force.

EXPERIMENTAL SECTION

Materials. 6-Mercapto-1-hexanol (MCH), hexaammineruthenium(III) chloride ($[\text{Ru}(\text{NH}_3)_6]^{3+}$), 4-(2-hydroxyethyl)piperazine-1-ethanesulfonic acid (HEPES), and tris(2-carboxyethyl)phosphine hydrochloride (TCEP) were purchased from J&K Scientific, Ltd. and used as received. Ethylenediaminetetraacetic disodium salt (Na_2EDTA), magnesium chloride hexahydrate, and sodium chloride were purchased from Beijing Chemical Co., Ltd. All other reagents were of analytical grade. The oligonucleotides were synthesized by Sangon Biotech (Shanghai) Co., Ltd. (Shanghai, China) and purified by HPLC; their sequences are listed in Table S1, Supporting Information. The capture probe was dissolved in immobilization buffer (“I-buffer”: 10 mM Tris-HCl, 10 mM TCEP, 0.5 M NaCl, pH 7.4) for 1 h before use, to ensure the absence of probe dimers. All solutions were prepared with Milli-Q water ($18.2 \text{ M}\Omega \text{ cm}^{-1}$) from a Millipore system.

Gel Electrophoresis. All the hairpin oligonucleotides were heated to 95 °C for 10 min before use to ensure the absence of dimers. Auxiliary DNA 1 (AD1, 2 μM) was incubated with Auxiliary DNA 2 (AD2, 2 μM) for 3 h in hybridization buffer (“H-buffer”: 10 mM Tris-HCl, 0.5 M NaCl, pH 7.4) before gel electrophoresis analysis. The agarose gel concentration was 1%, prepared by using 1× TAE buffer. The agarose gel electrophoresis was run at 50 V/10 cm for 30 min, followed by visualization under UV light and photography with a digital camera.

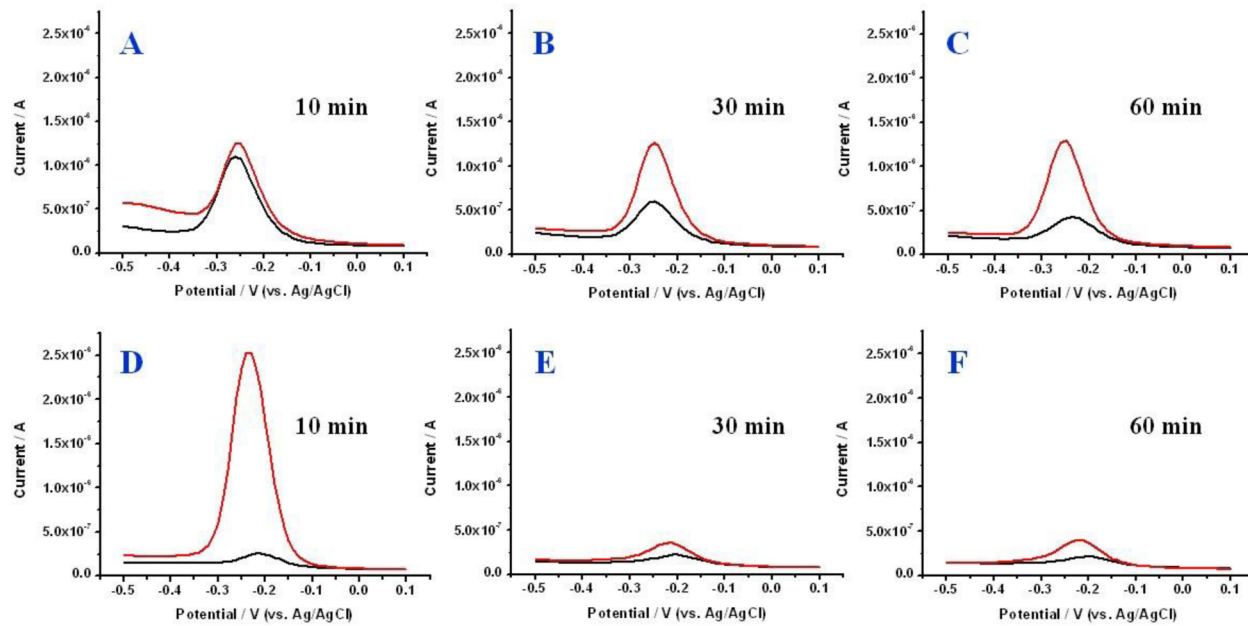


Figure 1. Optimization of the experimental conditions for the backfilling approach (A, B, and C) and the insertion approach (D, E, and F) at a fixed concentration of MCH ($50 \mu\text{M}$). The red and black lines represent the electrochemical signals corresponding to the capture probe and the DNA superstructure after assembly, respectively.

130 **Electrode Pretreatment.** The gold electrode (2 mm
131 diameter) was successively polished with 1.5, 0.5, and 0.05 μm
132 alumina slurries (Tianjin AidaHengsheng Technology Co., Ltd.)
133 until a mirror surface was formed. Then, the electrode was
134 sonicated in ultrapure water followed by ultrapure water and
135 ethanol (1:1 v/v) for 30 s each to remove the residual Al_2O_3
136 powder. After this treatment, the gold electrode was immersed in
137 freshly prepared piranha solution (1:3 v/v 30% $\text{H}_2\text{O}_2/\text{H}_2\text{SO}_4$)
138 for 10 min and thoroughly rinsed with distilled water. (Caution:
139 *piranha solution is highly caustic and must be used with care.*)
140 Finally, the electrode was cleaned by electrochemical polishing
141 with 30 successive cyclic voltammetry (CV) scans from +0.2 to
142 +1.6 V vs Ag/AgCl in 0.5 M H_2SO_4 at 50 mV/s.^{27–29} The
143 prepared electrode was rinsed with ultrapure water and dried
144 with nitrogen.

145 **Sensor Preparation.** The capture probe was freshly reduced
146 by mixing 2 μM of the probe with I-buffer for 1 h. For
147 heterogeneous monolayer preparation via the insertion
148 approach, the cleaned gold electrode was immersed in 50 μM
149 MCH solution for the proper time at room temperature,
150 followed by incubation in the DNA probe solution for 16 h at 4
151 °C. Thereafter, the electrode was rinsed thoroughly with the
152 washing buffer (“E-buffer”: 10 mM Tris-HCl, pH 7.4). For the
153 mixed monolayer derived from the backfilling approach, the
154 above process was reversed and the MCH occupied the free
155 interspaces between the DNA probes. The capture probe-
156 functionalized electrode was subsequently incubated with the
157 reaction buffer (50 mM HEPES, 100 mM NaNO_3 , pH 7.4)
158 containing different concentrations of Hg^{2+} for 1 h at 25 °C.
159 Then, after rinsing the electrode with the E-buffer, the electrode
160 was incubated with H-buffer containing 2 μM each of AD1 and
161 AD2 for 3 h at 25 °C. The electrode was again rinsed with the E-
162 buffer and dried with nitrogen before using for electrochemical
163 detection.

164 **Electrochemical Measurements.** For each point in the
165 calibration curve of electrochemical signal versus concentration,
166 four measurements were replicated on the same electrode. We

167 incubated the electrode modified with capture probes into the
168 reaction buffer containing different concentrations of Hg^{2+} for 1
169 h to form T- $\text{Hg}^{2+}\text{-T}$ complexes. Then, the electrode was
170 incubated in H-buffer containing 2 μM AD1 and AD2 for 3 h
171 to assemble the DNA superstructure, followed by a brief rinse
172 with E-buffer. The electrode with the assembled DNA
173 superstructure was immersed in the E-buffer containing 5 μM
174 [Ru(NH₃)₆]³⁺. The electrochemical measurements were per-
175 formed on an electrochemical workstation (CH Instruments,
176 Inc., Shanghai Chenhua Equipment, China) at room temper-
177 ature using a three-electrode system consisting of the
178 oligonucleotide-modified gold electrode as the working elec-
179 trode, a silver/silver chloride electrode (Ag/AgCl) as the
180 reference electrode, and a platinum wire as the counter electrode.
181 DPV was carried out in E-buffer within the potential range from
182 0.1 to -0.5 V with potential increments of 0.01 V. The amplitude
183 and pulse width were both 0.05 V, and the pulse period was 0.1 s.
184

185 **Electrochemical Detection of $\text{Hg}(\text{II})$ in Lake Water.** Lake
186 water was collected from Nanhui Park (Changchun, China) and
187 then filtered. Hg^{2+} was spiked into the lake water at different
188 concentrations (0, 1, 10, 100 nM) without dilution. The
189 electrochemical detection of Hg^{2+} was then performed in the
190 same manner as that used for the buffer samples.

■ RESULTS AND DISCUSSION

191 The maximum contour length of the DNA superstructure
192 assembled from two partial complementary DNAs can be more
193 than 1 μm .¹⁴ Once elongation is initiated on the surface,
194 sufficient free space is necessary for successful assembly. The
195 traditional DNA probe immobilization approach easily triggers
196 aggregation that leads to irreproducible results when combined
197 with DNA superstructures. The drawing in Scheme 1 illustrates
198 the insertion approach given by pathway A and the backfilling
199 approach represented by pathway B.

200 **DNA Superstructure Characterization via Agarose Gel**
201 **Electrophoresis.** The oligonucleotides were heated to 95° for
202 10 min before use. Lanes 1, 2, 3, and 4 in the 1% agarose gel were
203

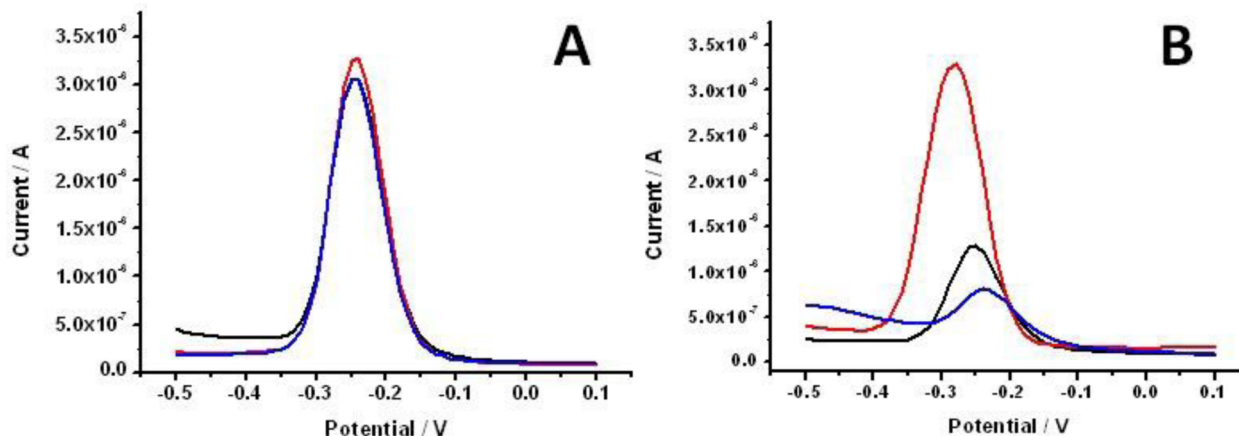


Figure 2. Reproducibility comparison between DPV signals via (A) the insertion approach and (B) the backfilling approach. Three independent experiments for each approach were carried out.

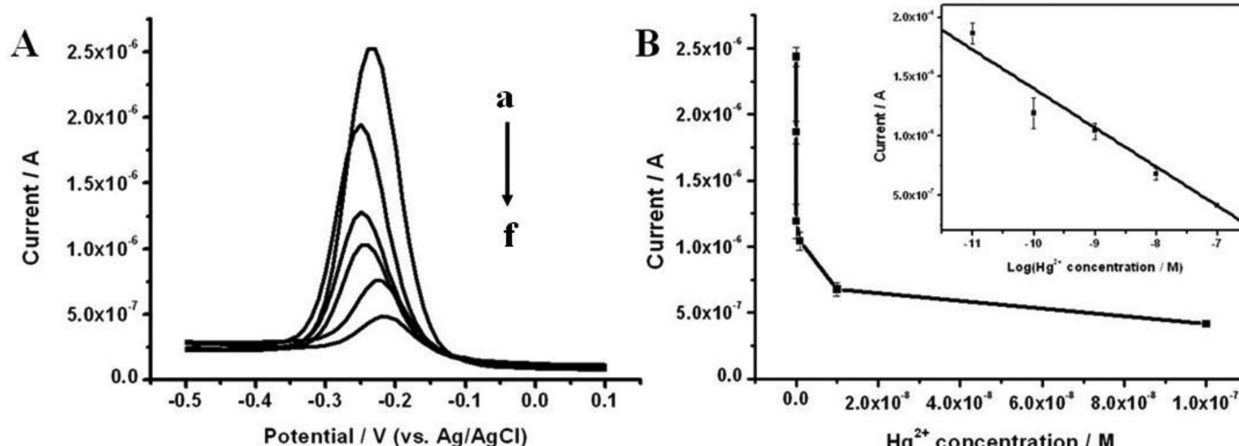


Figure 3. (A) DPV curves of various DNA superstructures assembled on the electrode in the presence of different amounts of Hg^{2+} (from a to f: 0, 10 pM, 100 pM, 1 nM, 10 nM, and 100 nM, respectively). (B) Plots of peak current versus the Hg^{2+} concentration. Inset is the linear relationship between the peak current and the logarithm of the Hg^{2+} concentration. The illustrated error bars represent the standard deviation from four repetitive measurements.

203 loaded with AD1 ($2 \mu\text{M}$), AD2 ($2 \mu\text{M}$), a mixture of AD1 ($2 \mu\text{M}$)
204 and AD2 ($2 \mu\text{M}$), and a Trans 5K DNA marker, respectively. As
205 shown in Figure S1, Supporting Information, the bands in lanes 1
206 and 2 clearly indicate the absence of high molecular weight
207 constituents. Instead, the lane loaded with the mixture of AD1
208 and AD2 exhibits a continuous broad band that demonstrates a
209 wide distribution of DNA superstructures. Assembly over 3 h
210 allowed DNA superstructure formation with a maximum length
211 above 500 base pairs, which was shown to be sufficient for signal
212 amplification. The experimental conditions adopted for DNA
213 assembly in solution were the same as those used for assembly on
214 the electrode surface. Although the growth of the DNA
215 superstructure in buffer solution concurs with the assembly
216 process on the electrode, it has little influence on the
217 reproducible assembly of DNA superstructures on the gold
218 electrode.
219

Advantage of the Insertion Approach versus the Backfilling Approach. It has long been a concern that MCH addition into the preassembled DNA monolayer can displace the preexisting DNA probes tagged with thiol moieties and lead to irreproducible results. In the absence of signal amplification, the backfilling approach is good enough for many applications. However, for building a highly sensitive sensor, signal

amplification is necessary, which entails enough free space around the DNA probes to allow the subsequent assembly. Furthermore, reproducibility is also another important criterion for sensor quality. In our case, a DNA superstructure more than 100 nm long was assembled on the gold electrode in a way that the requisite space between the DNA probes was large enough to achieve sufficient length.

Initially, to find the best conditions for both approaches, we fixed the DNA probe concentration at $2 \mu\text{M}$ and adjusted the concentration and the immobilization time for MCH. As shown in Figure 1A–C, a more than 30 min immobilization of $50 \mu\text{M}$ MCH that backfilled the interspaces between the preassembled DNA probes provided higher electrochemical signal amplification than a 10 min immobilization. The failure to observe a distinct change in the peak current before and after DNA superstructure assembly meant that a 10 min immobilization (Figure 1A) was insufficient to remove the nonspecifically absorbed DNA probes. We also utilized 1 mM MCH, which has been routinely used in previous studies;^{14,30–33} the results are shown in the Supporting Information (Table S2 and Figure S2). Unfortunately, the electrochemical signal amplification (Figure S2, Supporting Information) did not appear to increase after DNA superstructure assembly. Furthermore, the reproducibility

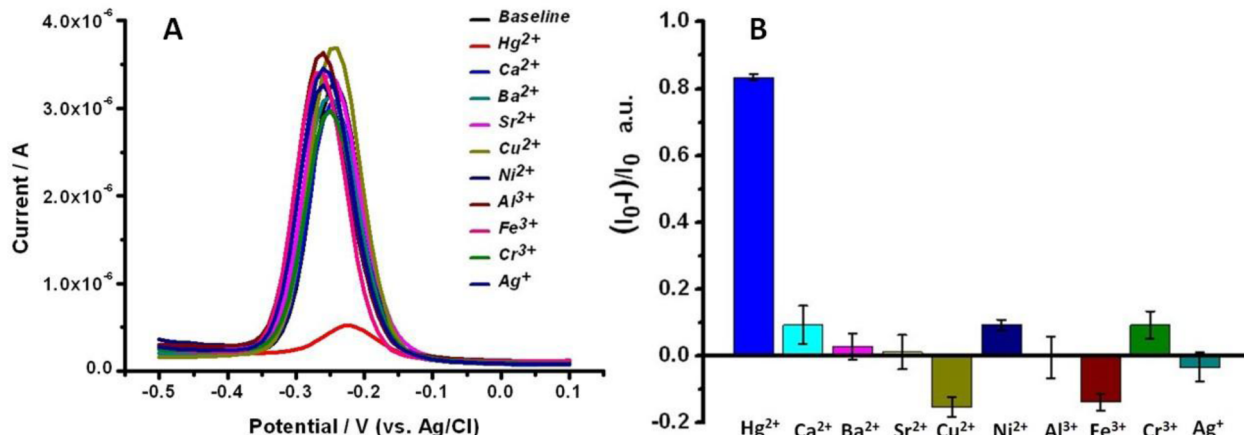


Figure 4. (A) DPV curves of various DNA superstructures assembled on the electrode in the presence of different metal ions. (B) Histograms of the peak currents of DPV curves of DNA superstructures in the presence of different metal ions. The concentration of each metal ion was both 100 nM. The illustrated error bars represent the standard deviation of four repetitive measurements.

249 based on the backfilling approach was much worse than previous
250 expectations would suggest, as demonstrated by Figure 2B.
251 Driven by the impetus to solve the poor reproducibility and
252 worse signal amplification problems posed by the backfilling
253 approach, the insertion approach, which has been shown to allow
254 sufficient space between DNA probes, was very appealing. As
255 shown in Figure 1D, the electrochemical signal amplification
256 corresponding to the difference in the peak currents was the
257 largest with a 10 min immobilization in 50 μ M MCH. According
258 to the chronocoulometry method (Figure S3, Supporting
259 Information) under the same experimental conditions, the
260 DNA surface densities with the insertion approach and
261 backfilling approaches are 1.03152×10^{12} and 2.4156×10^{12}
262 molecules/cm², respectively. For longer immobilization times,
263 the efficiencies of DNA probe binding and the subsequent DNA
264 superstructure assembly were significantly suppressed. The
265 number of defect sites after monolayer assembly was critical to
266 the amount of the immobilized DNA probes via the insertion
267 approach. Longer immobilization times (Figure 1E,F) and a
268 higher concentration of MCH (Figure S2D, Supporting
269 Information) were not favorable for this approach. By comparing
270 the two approaches under the same experimental conditions
271 (Figure 2A,B), it can be concluded that the reproducibility of the
272 insertion approach was much superior to the backfilling
273 approach.

274 **Electrochemical Detection of Hg^{2+} .** The electrochemical
275 detection of Hg^{2+} was performed by incubating the capture
276 probe-modified gold electrode for 1 h in aqueous solutions of
277 Hg^{2+} with defined concentrations. After the DNA probes folded
278 into loop structures via the formation of T- Hg^{2+} -T, the electrode
279 was incubated in a DNA solution containing AD1 and AD2. The
280 free DNA probes on the gold electrode acted as seeds to initiate
281 DNA assembly on the surface. The assembly process occurred
282 simultaneously on the electrode and in solution. By using
283 $[Ru(NH_3)_6]^{3+}$ as a signaling molecule that could bind to the
284 anionic phosphates of the DNA strands through electrostatic
285 interactions, the DPV peak current was used to quantitate the
286 Hg^{2+} concentration. As the Hg^{2+} concentration increases (Figure
287 3A), the DPV peak current correspondingly decreases. As shown
288 in Figure 3B, the calibration curve at target ion concentrations
289 from picomolar to submicromolar shows a linear relationship
290 between the current peak and the log value of the Hg^{2+}
291 concentration. A limit of detection (LOD) and limit of

292 quantification (LOQ) as low as 0.3 and 9.5 pM, respectively,
293 could be obtained based on this insertion approach. Although the
294 absolute value of the voltage corresponding to the peak current
295 decreased, this feature did not degrade the quality of our sensor
296 that combines the insertion approach and with signal
297 amplification via DNA superstructure formation.
298

299 **Selectivity of Hg^{2+} Detection.** The specificity of this sensor
300 for Hg^{2+} detection was evaluated using a variety of environ-
301 mentally relevant metal ions, including Ca^{2+} , Ba^{2+} , Sr^{2+} , Cu^{2+} ,
302 Ni^{2+} , Al^{3+} , Fe^{3+} , Cr^{3+} , and Ag^+ . We first investigated whether
303 these metals could individually influence the detection sensitivity
304 of Hg^{2+} . As shown in Figure 4A, the peak currents in the DNA
305 superstructures showed no change in the absence or presence of
306 other metal ions. The other metal ions presented only slight or
307 negligible effects on the peak current of this sensor's detection
308 system, indicating its outstanding specificity and selectivity
309 (Figure 4B) for Hg^{2+} against other metal ions.
310

311 **Recovery in Sample Analysis.** To investigate whether this
312 method was applicable to natural samples, we tested lake water
313 spiked with three different concentrations of Hg^{2+} : 1, 10, and 100
314 nM. Possibly interfering materials present in the lake samples did
315 not influence Hg^{2+} detection via the described method. As shown
316 in Table S3, Supporting Information, the recovery of Hg^{2+} from
317 spiked lake water samples demonstrates that the detection of
318 Hg^{2+} in natural waters is quite feasible. Therefore, this sensor
319 may be of great value for Hg^{2+} assays in real sample applications.
320

CONCLUSIONS

321 In this study, we adopted the insertion approach instead of the
322 backfilling approach to build up an electrochemical sensor. We
323 demonstrated that the insertion approach significantly improves
324 the reproducibility of electrochemical signal amplification via
325 DNA superstructure assembly. Using the detection of Hg^{2+} as a
326 prototypical example, we demonstrated that DPV could
327 quantitatively confirm the presence of Hg^{2+} . LOD and LOQ
328 values as low as 0.3 and 9.5 pM, respectively, were achieved.
329 Furthermore, excellent selectivity and real sample analysis
330 demonstrate the system's promising potential in future
331 applications. Other targets such as small molecules, DNAs, and
332 proteins might also be detected by the combination of the
333 insertion approach and signal amplification via DNA super-
334 structure assembly. Along with our results based on the

334 combination of the insertion approach and rolling circle
335 amplification (Figures S4–S7, Supporting Information), we
336 can envision many potential applications of this method beyond
337 the scope of this study, including its integration with other
338 amplification systems that require sufficient spacing.

339 ■ ASSOCIATED CONTENT

340 ■ Supporting Information

341 Additional information as noted in text. This material is available
342 free of charge via the Internet at <http://pubs.acs.org>.

343 ■ AUTHOR INFORMATION

344 Corresponding Authors

345 *E-mail: jhwang@ciac.jl.cn. Homepage: <http://nanopore.weebly.com/>.

347 *E-mail: liguijuan@mail.ccut.edu.cn.

348 *E-mail: ekwang@ciac.jl.cn.

349 Notes

350 The authors declare no competing financial interest.

351 ■ ACKNOWLEDGMENTS

352 This work was supported by grants from the National Natural
353 Science Foundation of China (Nos. 21190040 and 21275137),
354 the Start-up Fund of the Changchun Institute of Applied
355 Chemistry (CAS), and the Support Fund for Creative Young
356 Scientists (CAS).

357 ■ REFERENCES

- 358 (1) Seeman, N. C. *J. Theor. Biol.* **1982**, *99*, 237–247.
- 359 (2) Drummond, T. G.; Hill, M. G.; Barton, J. K. *Nat. Biotechnol.* **2003**,
360 *21*, 1192–1199.
- 361 (3) Fan, C. H.; Plaxco, K. W.; Heeger, A. J. *J. Proc. Natl. Acad. Sci. U.S.A.*
362 **2003**, *100*, 9134–9137.
- 363 (4) Herne, T. M.; Tarlov, M. J. *J. Am. Chem. Soc.* **1997**, *119*, 8916–
364 8920.
- 365 (5) Josephs, E. A.; Ye, T. *J. Am. Chem. Soc.* **2012**, *134*, 10021–10030.
- 366 (6) Josephs, E. A.; Ye, T. *Nano Lett.* **2012**, *12*, 5255–5261.
- 367 (7) Chen, X.; Hong, C. Y.; Lin, Y. H.; Chen, J. H.; Chen, G. N.; Yang,
368 H. H. *Anal. Chem.* **2012**, *84*, 8277–8283.
- 369 (8) Gong, P.; Levicky, R. J. *Proc. Natl. Acad. Sci. U.S.A.* **2008**, *105*,
370 5301–5306.
- 371 (9) Pei, H.; Lu, N.; Wen, Y. L.; Song, S. P.; Liu, Y.; Yan, H.; Fan, C. H.
372 *Adv. Mater.* **2010**, *22*, 4754–4758.
- 373 (10) Peterson, A. W.; Heaton, R. J.; Georgiadis, R. M. *Nucleic Acids Res.*
374 **2001**, *29*, 5163–5168.
- 375 (11) Ricci, F.; Lai, R. Y.; Heeger, A. J.; Plaxco, K. W.; Sumner, J. J.
376 *Langmuir* **2007**, *23*, 6827–6834.
- 377 (12) Wong, I. Y.; Melosh, N. A. *Nano Lett.* **2009**, *9*, 3521–3526.
- 378 (13) Joseph, E. A.; Ye, T. *ACS Nano* **2013**, *7*, 3653–3660.
- 379 (14) Adam, B. S.; Tonya, M. H.; Michael, J. T. *Anal. Chem.* **1998**, *70*,
380 4670–4677.
- 381 (15) Hylander, L. D.; Goodsrite, M. E. *Sci. Total Environ.* **2006**, *368*,
382 352–370.
- 383 (16) Zahir, F.; Rizwi, S. J.; Haq, S. K.; Khan, R. H. *Environ. Toxicol.*
384 *Pharmacol.* **2005**, *20*, 351–360.
- 385 (17) Zheng, N.; Wang, Q. C.; Zhang, X. W.; Zheng, D. M.; Zhang, Z.
386 S.; Zhang, S. Q. *Sci. Total Environ.* **2007**, *387*, 96–104.
- 387 (18) Erxleben, H.; Ruzicka, J. *Anal. Chem.* **2005**, *77*, 5124–5128.
- 388 (19) Thompson, M.; Coles, B. J. *Anal.* **1984**, *109*, 529–530.
- 389 (20) Chen, Y. W.; Tong, J.; D'Ulivo, A.; Belzile, N. *Analyst* **2002**, *127*,
390 1541–1546.
- 391 (21) Li, Y. K.; Xu, Y. R.; Huang, Y.; Dai, Y.; Hu, Q. F.; Yang, G. Y. *Asian*
392 *J. Chem.* **2009**, *21*, 2893–2897.
- 393 (22) Bings, N. H.; Bogaerts, A.; Broekaert, J. A. C. *Anal. Chem.* **2006**,
394 *78*, 3917–3945.

- (23) Han, F. X. X.; Patterson, W. D.; Xia, Y. J.; Sridhar, B. B.; Su, Y. *Water, Air, Soil Pollut.* **2006**, *170*, 161–171. 395
- (24) Zhang, L.; Chang, H. X.; Hirata, A.; Wu, H. K.; Xue, Q. K.; Chen, M. W. *ACS Nano* **2013**, *7*, 4595–4600. 397
- (25) Liu, S. J.; Nie, H. G.; Jiang, J. H.; Shen, G. L.; Yu, R. Q. *Anal. Chem.* **2009**, *81*, 5724–5730. 399
- (26) Tang, X. M.; Liu, H. X.; Zou, B. H.; Tian, D. B.; Huang, H. *Anal.* **2012**, *137*, 309–311. 401
- (27) Xiao, Y.; Lai, R. Y.; Plaxco, K. W. *Nat. Protoc.* **2007**, *2*, 2875–2880. 403
- (28) Yin, B. C.; Wu, D.; Ye, B. C. *Anal. Chem.* **2010**, *82*, 8272–8277. 404
- (29) Zhang, J.; Song, S. P.; Wang, L. H.; Pan, D.; Fan, C. H. *Nat. Protoc.* **2007**, *2*, 2888–2895. 405
- (30) Chen, Y.; Xu, J.; Su, J.; Xiang, Y.; Yuan, R.; Chai, Y. Q. *Anal. Chem.* **2012**, *84*, 7750–7755. 407
- (31) Lou, X. H.; Zhao, T.; Liu, R.; Ma, J.; Xiao, Y. *Anal. Chem.* **2013**, *85*, 409 7574–7580.
- (32) Yuan, T.; Liu, Z. Y.; Hu, L. Z.; Zhang, L.; Xu, G. B. *Chem. Commun.* **2011**, *47*, 11951–11953. 411
- (33) Zhu, Z. Q.; Su, Y. Y.; Li, J.; Li, D.; Zhang, J.; Song, S. P.; Zhao, Y.; Li, G. X.; Fan, C. H. *Anal. Chem.* **2009**, *81*, 7660–7666. 413
- (34) 414